Nanoscale Pulling of Type IV Pili of *Pseudomonas aeruginosa* PAO1 Reveals Their Flexibility and Adhesion to Surfaces over Extended Lengths of the Pili

Biophysical Journal

Supporting Material

Shun Lu,[1] Maximiliano Giuliani,[1] Hanjeong Harvey,[2] Lori L. Burrows,[2] Robert A. Wickham,[1] and John R. Dutcher[1]#

[1]Department of Physics, University of Guelph, Guelph, Ontario, Canada N1G 2W1

[2]Department of Biochemistry and Biomedical Science, McMaster University, Hamilton, Ontario, Canada L8N 3Z5

Correspondence: Address reprint requests to John Dutcher, Department of Physics, University of Guelph, Guelph, Ontario, Canada N1G 2W1; Tel: 519-824-4120, ext. 53950; Fax: 519-836-9967; Email: dutcher@uoguelph.ca

S1: AFM Imaging of Type IV Pili (T4P)

In Fig. S1, AFM images are shown for *P. aeruginosa* PAO1 *pilT* mutant cells, collected in air using contact mode. In these images, two different kinds of bacterial cell appendages can be seen: thicker (13-20 nm diameter) flagella, and thinner (~ 5 nm diameter) T4P. T4P on wild-type *P. aeruginosa* PAO1 cells are most clearly seen in the AFM deflection image in Fig. S1e. The AFM topography images were used to generate the line profiles in Fig. S1f-h. We note that some of the filaments in the AFM images are considerably thicker than individual T4P but thinner than flagella (Fig. S1a-c), and we interpret these as bundles of multiple T4P.

The *pilT* mutant cells typically had a large number of long (> 6 μm) T4P, for cells cultured on both agar plates and in TSB media (Fig. S1a). These pili are significantly longer than those on wild-type *P. aeruginosa* PAO1 cells grown on either 1% agar plates or cultivated in TSB media. The large number of long T4P observed for the *pilT* mutant strain is due to the high level expression of the PilA protein, which is the major pilin subunit of T4P in *Pseudomonas* due to induction of *pilA* expression with 0.2% L-arabinose (11). Deletion of *pilT* prevents retraction, giving rise to longer T4P on average than observed for wild-type cells. Because of the lack of retraction of T4P in the *pilT* mutant, it was ideal for the AFM pulling study.

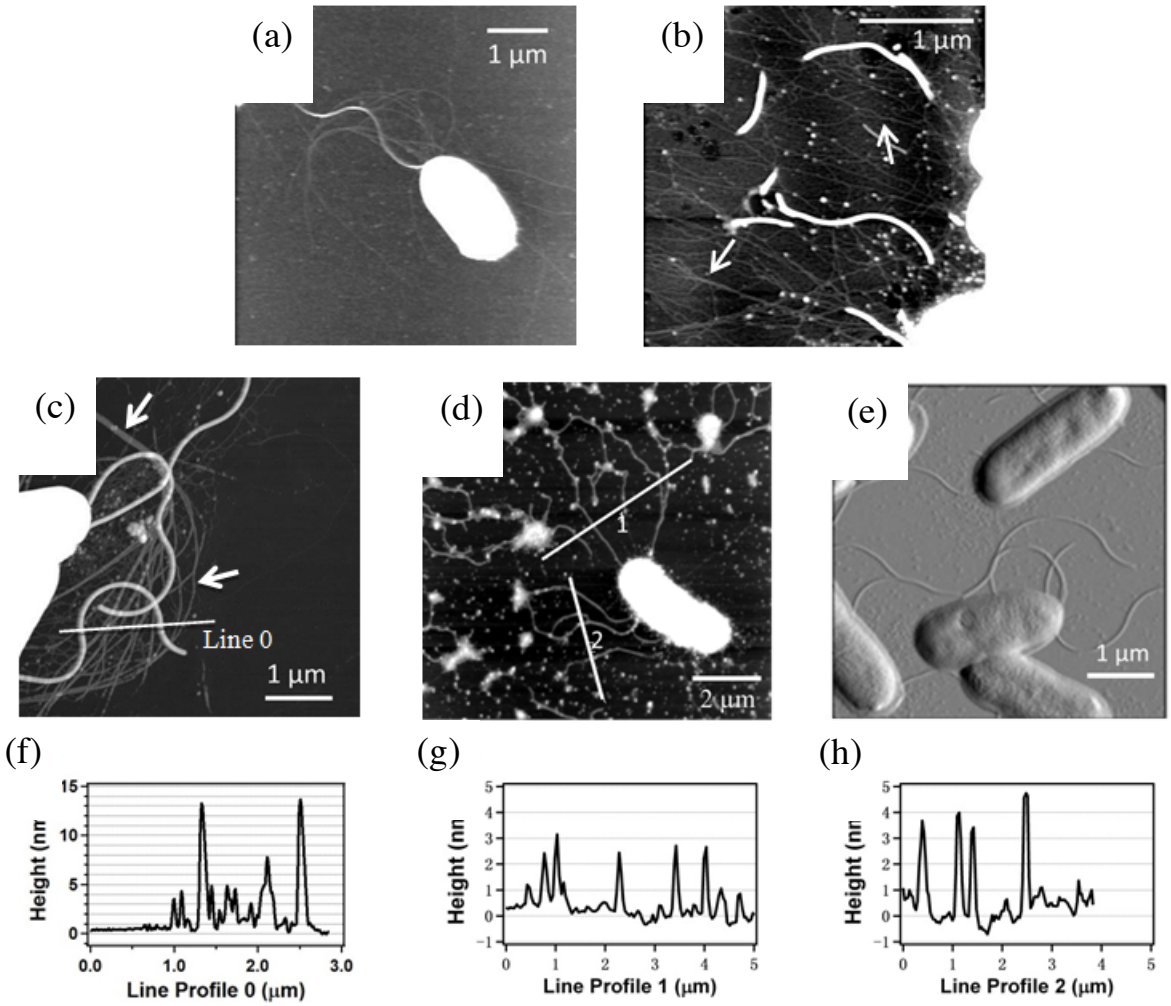

Figure S1: (a)-(e) AFM images of *P. aeruginosa* PAO1 *pilT* mutant bacterial cells deposited onto mica, measured in contact mode in air. (a-d) correspond to topography images, and (e) corresponds to a deflection image. (a) *pilT* mutant cell, grown in TSB medium plus gentamicin. (b) T4P of *pilT* mutant cells, with bundles indicated by white arrows. (c) T4P of *pilT* mutant cells, together with larger diameter flagella. The lower arrow points to isolated T4P, and the upper arrow points to T4P that are bundled along part of their length. (d) *fliC* mutant bacterial cells with T4P but no flagella. (e) *P. aeruginosa* PAO1 wild-type cells grown in LB medium. (f)-(h) Line profiles along line 0 in (c), and lines 1 and 2 in (d), showing that the T4P have heights of 2-6 nm, and flagella have heights of 13-15 nm.

S2: Statistical Model of Mechanical Pulling of a Type IV Pilus (T4P) Adsorbed to a Surface

The AFM force pulling experiment is statistical in nature and samples an ensemble of T4P conformations. In this section we develop a statistical model to understand the physics behind the existence of plateaus in the AFM force-separation curves (Fig. 5) and, in particular, to explain the observed distributions of plateau lengths (Fig. 6). Both the freely-jointed chain (FJC) and the worm-like chain (WLC) models of polymer physics should adequately describe the T4P, since in all cases examined the persistence length, L_p, is much smaller than the contour length, L_c, of the T4P. We consider a freely joined chain of N links, where each link has a Kuhn length a that is approximately twice the persistence length of the relaxed T4P, i.e. $a = 2L_p$. Since the contour length $L_c = Na$ is typically on the order of several microns, N is typically on the order of 10^2. For a single T4P partially adsorbed to the surface, the situation is shown schematically in Fig. S2. The pilus can be considered as consisting of two distinct segments: segment 1, which is a chain of n links stretching between the AFM tip and the surface, and under tension f in the surrounding liquid above the surface; and segment 2, which is the adsorbed portion of the pilus with $N - n$ links. This situation would lead to a plateau of length $L = (N - n)a$ in an AFM force-separation curve.

We now consider all chain conformations of the pilus, at fixed N, n, f, and temperature T, each conformation weighted by the equilibrium Boltzmann weight, and we compute the single-pilus partition function. A similar calculation for a single chain partially adsorbed to a surface was presented in Ref. S1. The partition function $Q_1(n)$ for segment 1 of the chain can be written as:

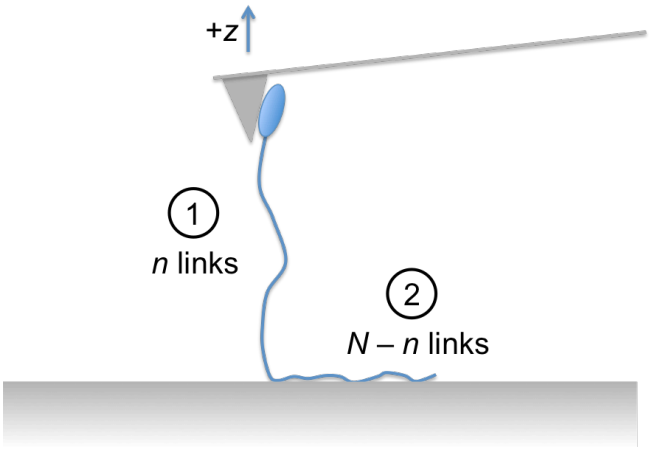

Figure S2: Schematic diagram of AFM pulling on a T4P of N Kuhn segments of length a, with n links under tension f in the surrounding liquid and (N - n) links adsorbed onto the underlying surface. We assume that the T4P are pulled vertically (+z-direction) into the liquid from the interface, with the adsorbed segments sliding freely on the surface.

$$Q_1(n) = \prod_{i=1}^{n} \int d\Omega_i e^{-\beta f a \sum_i \cos\theta_i} = \left[\frac{4\pi \sinh(\beta f a)}{\beta f a}\right]^n \quad , \qquad \text{(S1)}$$

where $\beta = 1/k_B\mathrm{T}$, $d\Omega_i$ is the differential solid angle into which the tangent vector $\vec{t_i}$ of the i^{th} link points, and $fa\sum_i \cos\theta_i$ is the work performed by pulling the chain with force f in the liquid ($\hat{z} \cdot \vec{t_i} = a\cos\theta_i$). The partition function for segment 2 of the chain is

$$Q_2(N-n) = \prod_{i=1}^{N-n}\left[\int_0^{2\pi} d\theta_i e^{\beta\varepsilon a}\right] = (2\pi)^{N-n} e^{\beta\varepsilon a(N-n)} \quad , \qquad \text{(S2)}$$

where θ_i is the angle in the plane of the surface made by the i^{th} link relative to some axis, and $-\varepsilon a$ is the energy of adsorption of a link onto the surface. A key quantity of interest is ε, the adhesion energy per unit length between the T4P and the surface. The partition function for the whole pilus, at fixed N, n, f, and T, is then

$$Q(N,n) = Q_1(n)Q_2(N-n) = (2\pi)^N e^{\beta\varepsilon aN} e^{\mu n}, \qquad \text{(S3)}$$

where

$$\mu \equiv \ln\left[\frac{2\sinh(\beta f a)}{\beta f a}\right] - \beta\varepsilon a. \qquad \text{(S4)}$$

Equations S1-S4 describe the partition function for a single pilus, however the AFM pulling experiments sample an ensemble of T4P, with various N and n. We will consider the ensemble of T4P for which the AFM force-separation curves have a force plateau. We will assume that, for a given surface material, the tension f in segment 1 of the pilus, which we take to be the plateau force, is the same for each T4P in the ensemble. In the experiments, there is a distribution of plateau forces (Fig. 7) for T4P in the ensemble, but if the distribution is narrow (as it is for the gold surface, Fig. 7b, and, to a lesser degree, for the mica surface, Fig. 7a), we expect this assumption to be reasonable. Therefore, we work in an ensemble where f and T are fixed, but where N and n are different for each pilus in the ensemble. We take the distribution of T4P contour lengths, $P(N)$, to be similar to the rupture length distributions (Fig. 2) and we can

use this weighting of the polydispersity in the pilus length in our definition of the partition function, Z, of the ensemble of T4P at temperature T and having a plateau force f:

$$Z = \sum_{N=0}^{\infty} P(N) \sum_{n=0}^{N} Q(N,n) \quad . \qquad \text{(S5)}$$

The experiments measure averages over T4P in the ensemble, which are calculated using

$$\langle ... \rangle \equiv \frac{1}{Z} \sum_{N=0}^{\infty} P(N) \sum_{n=0}^{N} (...) Q(N,n) \quad . \qquad \text{(S6)}$$

The key average quantity to calculate is the plateau length distribution, $W(L)$, which is proportional to the number of T4P, at fixed f and T, that have $N - n = L/a$ links adsorbed to the surface. The plateau length distribution is given by

$$W(L) \equiv \left\langle \delta_{L/a,(N-n)} \right\rangle = \frac{1}{Z} \sum_{N=L/a}^{\infty} P(N) Q\left(N, N - \frac{L}{a}\right) , \qquad \text{(S7)}$$

where δ is the Kronecker delta that forces $N - n = L/a$ for T4P in the ensemble. We use equations S3 and S4 to write the plateau length distribution as

$$W(L) = e^{-\mu L/a} \frac{1}{Z} \sum_{N=L/a}^{\infty} P(N) \left[\frac{4\pi \sinh(\beta f a)}{\beta f a} \right]^N . \qquad \text{(S8)}$$

The L-dependence of $W(L)$ comes through the exponential decay, and through the lower limit of the sum in equation S8. Provided that L/a is much less than the upper limit on N dictated by $P(N)$, we can replace the lower limit of the sum, $N = L/a$, by $N = 0$ with only a negligible difference to the result. The broad rupture length distributions (Fig. 2) drop off significantly for large values of L_c, but from Fig. 6 we see that it is highly unlikely to have force plateaus longer than several microns. Thus we are justified in replacing the lower limit of the sum in equation S8 with $N = 0$. This leads to the conclusion, supported by the data in Fig. 6, that the plateau length distribution follows an exponential decay law:

$$W(L) \propto e^{-L/L_d}, \qquad \text{(S9)}$$

with a decay length L_d given by

$$\frac{L_d}{a} = \frac{1}{\mu} = \frac{1}{\ln\left[\frac{2\sinh(\beta f a)}{\beta f a} \right] - \beta \varepsilon a} . \qquad \text{(S10)}$$

The constant of proportionality in equation S9 can be determined from the normalization of $W(L)$, if desired. Our model suggests that the plateau length distribution is insensitive to the

form of the pilus contour length distribution, provided that the distribution is rather broad and featureless.

Using the values of the plateau decay length, the plateau force, and the Kuhn length of our T4P determined from our experiments, we can use equation S10 to calculate ε, the adhesion energy per unit length of T4P to a surface. In our experiments, $L_d/a \sim 50 \gg 1$, and $\beta f a \gg 1$ (for example, for f = 200 pN, $\beta f a \approx 900$), so we can approximate equation S10 as

$$\beta \varepsilon a \approx \beta f a - \ln(\beta f a). \qquad \text{(S11)}$$

Therefore, the adhesion per unit length of T4P on the surface is very nearly equal to the measured plateau force.

S3: Effect of Non-zero Pulling Angle on Measured Persistence Length of T4P

Since the lengths of the T4P are comparable to the maximum vertical separation (~ 10 μm) in our force-separation curves and since adsorbed T4P segments will likely not be able to slide on surfaces, the assumption that we pull vertically on the T4P is not necessarily valid. Therefore, we need to consider the effect of a lateral offset between the points of contact between the T4P and the AFM cantilever and sample surface (S2-S4). We can redefine our experimental schematic geometry by allowing for a non-zero attachment angle ϕ, as shown in Figure S3. The vertical distance R_z between the AFM cantilever and the surface and the lateral distance R_x can be combined to give the total distance R between the cantilever and the contact

point as $R = \sqrt{R_z^2 + R_x^2}$. In the presence of a vertical external force F_z exerted on the T4P by the AFM cantilever, the equilibrium extension of the T4P at constant speed is obtained by minimizing the free energy with respect to displacement in the vertical direction. A geometric factor α can be defined that is related to the orientation of the T4P with respect to the vertical *z*-direction (Fig. S3), and is defined as $\alpha = 1/\cos\phi = \sqrt{1 + R_x^2/R_z^2} = (1 - R_x^2/R^2)^{-1/2}$. For a worm-like chain with persistence length L_p in the large-stretching limit, the force-distance relation is given by $\frac{4L_p \alpha F_z}{k_B T} = \left(1 - \frac{\alpha R_z}{R}\right)^{-2}$ (S2). The geometric factor α can be understood as a renormalization factor for the persistence length L_p and the distance R between the cantilever and the contact point. For a polymer chain executing a self-avoiding random walk on the surface, the value of α is determined by the values of L_p and R according to $\alpha \approx 1 + \frac{1}{2}\left(\frac{2L_p}{R}\right)^{1/2}$ (S2). Given the small values of L_p measured in the present experiments (< 50 nm, as can be seen in Fig. 3) and the large values of the T4P contour length (~ 5 μm), the geometric factor α < 1.07, which produces only small corrections to our measured L_p values due to the non-zero pulling angle.

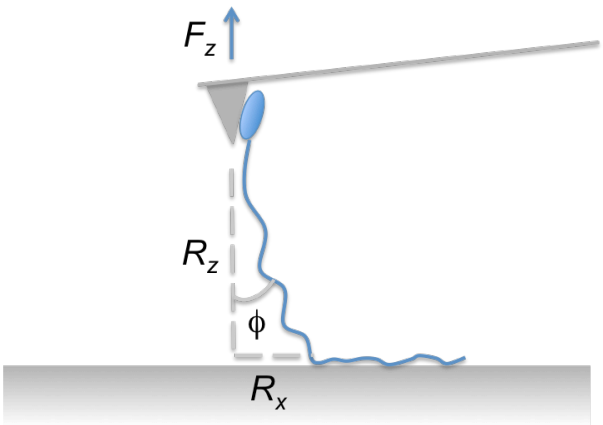

Figure S3: Schematic geometry of a T4P pulling experiment for a single T4P and a non-zero attachment angle ϕ. A segment *S* of the T4P is adsorbed onto the underlying surface, and it is detached from the surface

by a vertical pulling force F_z exerted on the T4P by the retracting AFM cantilever. During the pulling process, the contact point shifts laterally on the surface as the adsorbed segment is removed from the surface.

S4: Effect of T4P Flexibility on the Uncertainty in the Best-Fit Values of the T4P Rupture and Persistence Lengths

The AFM force pulling experiments in the present study showed that T4P are very flexible, with best-fit persistence length values for single, relaxed T4P of either $L_p \sim 1$ nm (if T4P remain intact at high pulling forces) or $L_p \sim 9$ nm (if isolated strands are formed at high pulling forces). In either case, the T4P are highly flexible, such that, in the absence of motion of the cell, they are well described by a random coil tethered to the bacterial cell surface. For a T4P of length 10 μm with a Kuhn length a that is approximately twice the persistence length of the relaxed T4P, i.e. $a = 2L_p$, the number of repeat units is either $N \sim 5000$ (for $L_p \sim 1$ nm) or N ~ 500 (for $L_p \sim$ 9 nm). For a random coil, the root-mean-square end-to-end distance is $\sim L_p N^{1/2}$, which yields a value of either ~ 70 nm or ~ 200 nm, both of which are significantly less than the fully extended contour length of the T4P. The small extent of the T4P from the bacterial cell wall means that cells must be very close to a surface for the T4P to adhere to the surface. Because of this, only cells adhered close to the apex of the pyramidal tip will contribute to T4P pulling curves. This means that the uncertainty in the value of the rupture length of the T4P stretched between the AFM cantilever and the underlying surface is small (maximum uncertainty of ± 100 nm). This produces a correspondingly small uncertainty in the best-fit persistence length values.

S5: T4P Pulling Experiments Using Colloidal AFM Tips

We also performed T4P pulling experiments using silicon nitride AFM cantilevers with a

600 nm diameter colloidal tip. The use of the colloidal tips reduced the distance between the underside of the cantilever and the underlying mica surface such that it was comparable to the diameter of the bacterial cells, ensuring that the cells were close to, but not in contact with, the mica surface. SEM images of AFM cantilevers with a sharp pyramidal tip and a colloidal tip are shown in Figure S4, in which it can be seen that the size of the tip is dramatically smaller than that of the sharp pyramidal AFM tips, but also that the number of bacterial cells adhered to the AFM cantilever was also much smaller (cf. Fig. S4a and b).

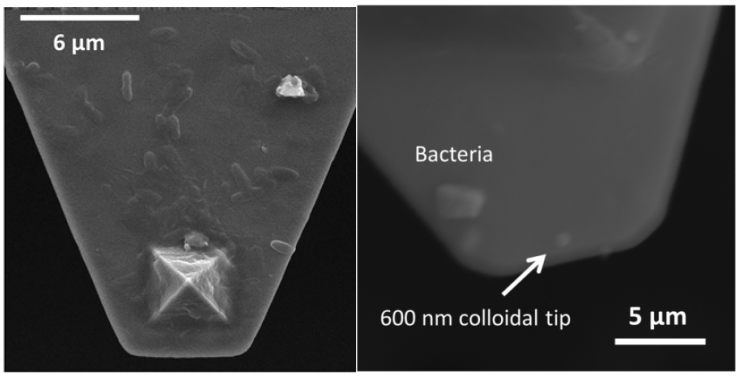

Figure S4: Scanning electron microscopy (SEM) images of the end of silicon nitride AFM cantilevers with (a) a sharp pyramidal tip and (b) a 600 nm diameter SiO_2 colloidal tip. *P. aeruginosa* PAO1 *pilT* mutant bacterial cells have been adhered using poly-L-lysine onto the base of each cantilever. Fewer cells are adsorbed onto the cantilever with the colloidal tip.

Histograms of the persistence length L_p, the rupture force and the rupture length measured using the 600 nm colloidal tips on mica surfaces are shown in Fig. S5. The rupture force histogram in Fig. S5 has a single peak at 80 pN, which is comparable to the main peak at 90 pN in the corresponding rupture force distribution measured on mica surfaces using a sharp AFM tip (Fig. 2d). The observation of single peaks in the two histograms at approximately the same value of the rupture force allows us to infer that the fundamental adhesion force between the

T4P and the mica surface is ~ 80 pN. The rupture force peak that is observed at ~ 160 pN for the sharp AFM tip and the mica surface (Fig. 2d) is possibly due to contact between a bundle of two T4P and the mica surface. The L_p distribution measured using the colloidal AFM tips (Fig. S5a) has a primary peak at 1.4 nm and a tail to higher values of L_p, with perhaps a very small secondary peak at 5.5 nm. The absence of higher order peaks in the L_p distribution and the secondary peak in the rupture force are consistent with a lower frequency of T4P bundling for the measurements performed using AFM cantilevers with colloidal tips, which is probably due to the smaller number of cells adhered to these cantilevers than for the cantilevers with sharp, pyramidal tips. The rupture length distribution measured using the colloidal AFM tips (Fig. S5c) has more rupture events below 2 μm for the colloidal tips than for the pyramidal sharp tips.

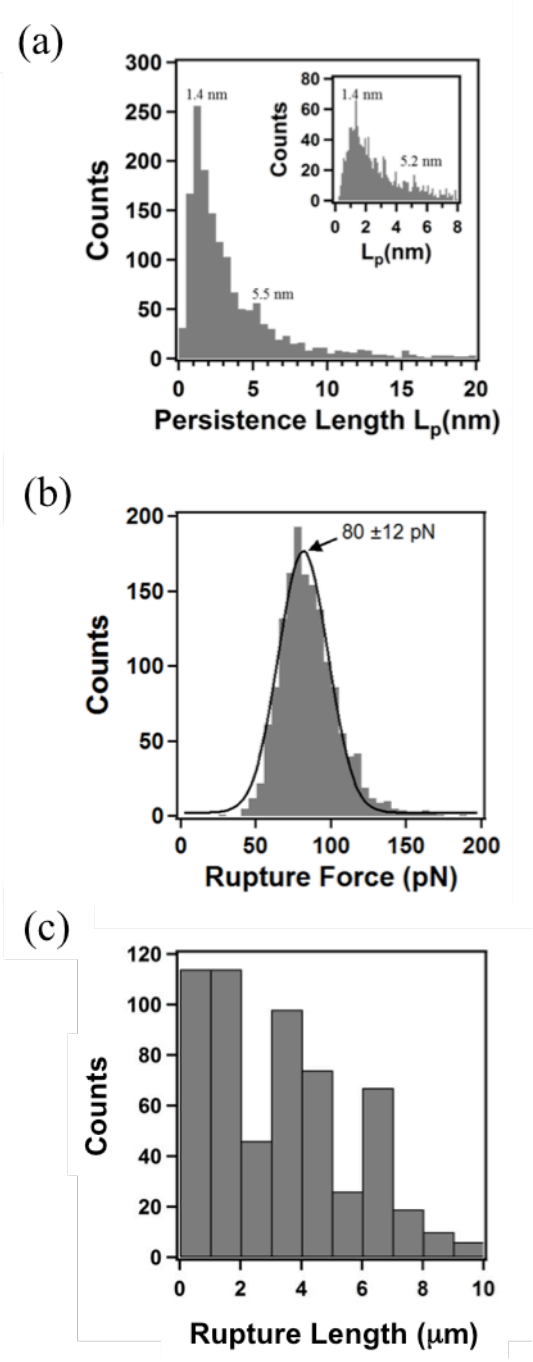

Figure S5: (a) Histogram of persistence length (bin size = 0.5 nm) measured by pulling of T4P of a *P. aeruginosa* PAO1 *pilT* mutant strain measured during retraction of AFM cantilevers with a 600 nm colloidal tip from a mica surface. The inset is an expanded view of the L_p distribution from 0 to 8.0 nm with a smaller bin size of 0.1 nm. (b) Histogram of the rupture force, obtained from the same set of force curves as that in

(a), showing a single force peak at 80 pN. (c) Histogram of the rupture lengths, obtained from the same set of force curves as in (a).

S6: Morphology of Mica, Gold and Polystyrene Surfaces

Three different surfaces (hydrophilic gold and mica, and hydrophobic polystyrene) were used as the underlying substrates for the AFM pulling experiments. AFM deflection images of the morphologies of these surfaces are shown in Fig. S6a-c. The freshly-cleaved mica surfaces were atomically flat; the flame-annealed gold (111) surfaces had well defined, atomically flat terraces with step height of several nanometers, and the polystyrene films had slightly larger surface roughnesses than the mica surfaces, but were quite smooth (RMS roughness ~ 0.4 nm over an area of 1 μm^2). Therefore, all of the substrates provided flat surfaces onto which T4P could adsorb for use in the AFM pulling experiments.

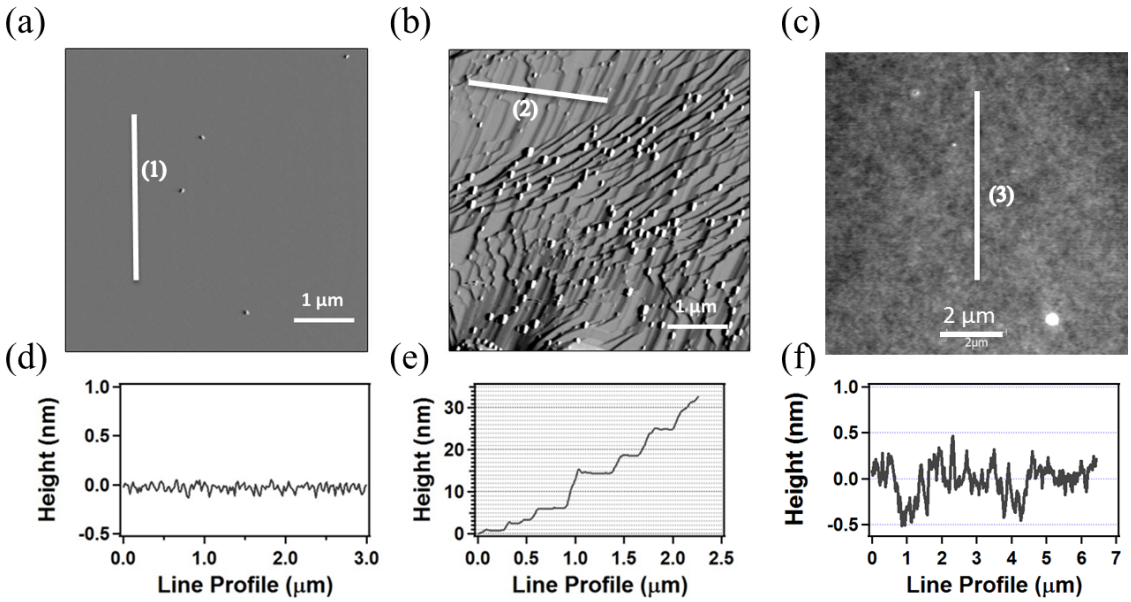

Figure S6: AFM deflection images of (a) freshly-cleaved mica, (b) flame-annealed gold, and (c) a spin-coated polystyrene film. (d-f) Line profiles along the white lines in the corresponding AFM topography images for (a-c), respectively.

Supporting References:

S1. **Iliafar S, Wagner K, Manohar S, Jagota A, Vezenov D.** 2012. Quantifying interactions between DNA oligomers and graphite surface using single molecule force spectroscopy. J. Phys. Chem. C **116:**13896-13903.

S2. **Serr A, Netz RR.** 2006. Pulling adsorbed polymers from surfaces with the AFM: stick vs. slip, peeling vs. gliding. Europhys. Lett. **73:**292-298.

S3. **Rivera M, Lee W, Ke C, Marszalek PE, Cole DG, Clark RL.** 2008. Minimizing pulling geometry errors in atomic force microscope single force spectroscopy. Biophys. J. **95:**3991-3998.

S4. **Ke C, Jiang Y, Rivera M, Clark RL, Marszalek PE.** 2007. Pulling geometry induced errors in single molecule force spectroscopy measurements. Biophys. J. **92:**L76-L78.